Q&P Heat Treatment of a FeCSiMn Steel

Robert B. Tuttle
Mujeeb H. Shaik
Western Michigan University, Kalamazoo, Michigan, USA

ABSTRACT

The specialized quench and partition (Q&P) heat treatment process appears to have broad application, including in cast products. This study investigates the response of a 0.25C-1.7Si-3.4Mn cast steel to different Q&P heat treatment cycles. A 25 mm thick Y-block casting provided a longer solidification time and diffusion distance than has been done in this alloy before. Smaller samples were extracted from the Y-block casting for heat treatment. These samples were then examined to determine their hardness, microstructure, and phase formation. X-ray diffraction (XRD) confirmed phase evolution and retained austenite carbon content. Data also suggests that the time lengths for the various Q&P stages must be longer for thicker sections to achieve the desired structures and properties.

Keywords: quench and partition, Q&P, medium manganese steels, heat treatment, retained austenite

INTRODUCTION

The quench and partition (Q&P) process is a novel heat treatment initially theorized by Speer et al. in 2003.[1] The goal of this heat treatment was to create a microstructure consisting primarily of martensite and retained austenite. The significant amount of retained austenite contained in these steels contributes to their unique microstructure and properties.[1] While the austenite is stable at room temperature, it transforms during plastic deformation into additional martensite. This change is called transformation induced plasticity (TRIP).[1,2] The resulting increase in martensite causes an increase in strength and additional elongation since the martensite transformation results in a larger volume of material.[1,2] Thus, the retained austenite in Q&P steels provides a higher ultimate tensile strength (UTS) and percent elongation.[1,3,4]

A schematic illustration of the quench and partition process can be observed in Figure 1 and is divided into three major steps.[5] The first step is austenitization which means the material is heated to form only austenite.[5] The second step is quenching. The austenitized steel is rapidly cooled between the M_s and M_f temperatures, which results in the desired amounts of martensite and retained austenite. The third step is partitioning, the quenched steel is reheated to the partitioning temperature and held for a specific period of time. The carbon from the supersaturated martensite diffuses into the austenite and enriches it. This stabilizes the austenite at room temperature and further enables the TRIP mechanism. The maximum amount of carbon enrichment that can be achieved during the partitioning cycle is governed by the constrained paraequilibrium (CPE) conditions in the alloy.[3] After this step, the material is allowed to cool to room temperature.

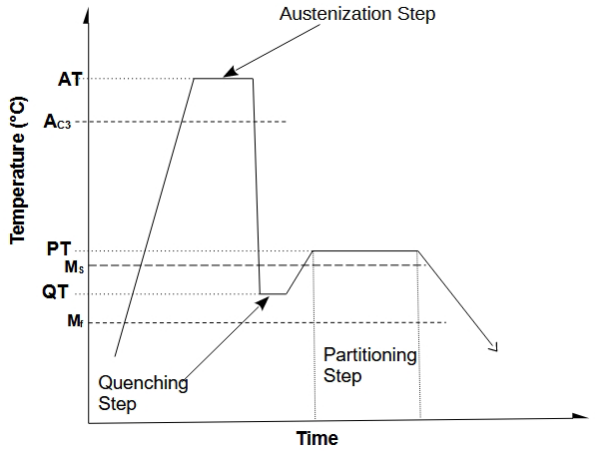

Figure 1. A schematic illustration of the Quench and Partition process (Q&P).

Originally developed for sheet metal applications, the Q&P process was tailored specifically for use in the automotive industry for body-in-white applications. However, the benefits of Q&P steels extend far beyond this application, resulting in diverse possibilities. This alloying and heat treatment approach means that these alloys could be applied in steel castings for the aerospace, defense, and trucking industries. The appeal of Q&P steels lies in their capacity for weight reduction coupled with high strength and good ductility. Notably different from conventional high-strength steels, Q&P steels offer a unique combination of strength and ductility. Traditional steels, in contrast, typically exhibit robust strength but lower ductility than what is found in Q&P steels. For example, 4140 quenched and tempered (Q&T) steel has a yield of 1035 MPa, UTS of 1140 MPa, with a percent

elongation of 5%. Work by Wendler at al. on a 15Cr-3Ni-3Mn-0.5Si-0.12N-0.16C Q&P steel , which is similar to 4140, shows a significant difference in the mechanical properties.[6] The mechanical properties were reported to be a yield of 1050 MPa, UTS of 1550 MPa, and a percent elongation of 22%.[6] Thus, the strength and percent elongation were higher in the Q&P steel. This trend for a higher ductility at higher strength levels has been found in other Q&P steel research.[6-15]

To take advantage of the Q&P process, the steel must be designed for the Q&P process. Speer developed a model to address carbon partitioning from as-quenched martensite into austenite, under conditions where competing reactions such as bainite, cementite, or transition carbide precipitation are suppressed.[1] In the absence of carbide formation, the CPE condition can be calculated based on straightforward thermodynamic and mass balance constraints.[1] First, carbon diffusion occurs when the chemical potential of carbon is unequal in ferrite and austenite, and ceases when they are even.[1] Ignoring effects of alloying on carbon activity, this requirement may be represented using the results of Lobo and Geiger for the Fe-C binary system as follows:[1,3,16,17]

$$X_C^{\gamma} = X_C^{\alpha}.e^{\frac{76{,}789-43.8T-(169{,}105-120.4T)X_C^{\gamma}}{RT}} \quad \text{Eqn. 1}$$

where $\boldsymbol{X_C^{\gamma}}$ and $\boldsymbol{X_C^{\alpha}}$ represent the mole fractions of carbon in austenite and ferrite. The relevant thermodynamics are embedded in Equation 1.[1,3] Equation 2 can be used to predict the M_s of the steel.

$$M_s(^{\circ}C) = 499 - 317(\%C) - 33(\%Mn) - 28(\%Cr) - 17(\%Ni) - 11(\%Si) - 11(\%Mo) - 11(\%W) \quad \text{Eqn. 2}$$

The martensite fraction (f_m) was predicted by using the Koistinen–Marburger Relationship, which relates the degree of undercooling below the M_s to the amount of martensite formed (Equation 3).

$$f_m = 1 - e^{-1.1x10^{-2}(\Delta T)} \quad \text{Eqn. 3}$$

where f_m is the volume fraction of the martensite and ΔT is the temperature difference between the Ms and the quench temperature.

The use of manganese and silicon in Q&P alloys occurs for several reasons. Both silicon and manganese are reported to stabilize austenite at room temperature.[1] Manganese promotes the formation of higher fractions of austenite which is crucial to achieve the desired microstructure. Silicon additions are made to suppress cementite precipitation which makes more carbon available for absorption by austenite. Thus, the retained austenite will be enriched with all the carbon that leaves the supersaturated martensite phase.[4] This enhances the steel's mechanical properties by ensuring phase stability and suppressing undesirable cementite precipitation, contributing to the improved properties of these alloys.

In prior research, the Q&P process has often been applied to rolled sheet metal products (< 1mm thick). Little information exists in the open literature regarding casting or thick section steel products. Heat treating larger section sizes for casting materials can present several challenges due to factors such as uneven heating and cooling rates, and internal stresses. Larger casting sections have more mass, requiring more time to heat or cool compared to smaller sections. Similarly, thicker sections will take longer to reach the desired temperature during heating and will require more time to cool down uniformly during quenching. Ferrite, being a soft phase in steel, can compromise the mechanical properties achieved in these steels. Longer times might cause the formation of ferrite.[4] The slower cooling rates of castings can result in carbide formation. Longer heating times are often necessary to dissolve these carbides completely into the matrix for thicker sections. In this study, a comprehensive examination of phase fractions, hardness, and microstructure characterization has been conducted across three distinct stages: the as-cast, quenched, and partitioned stages. The intent of the research was to determine if the Q&P process could be conducted on thicker samples (~ 12mm), determine the time required for the various heat treatment stages, and examine the microstructure evolution in a sand cast material.

EXPERIMENTAL PROCEDURE

A 25mm thick, 152mm height, and 178mm wide Y-block casting was employed in this experiment (Figure 2). Molds were made using a resin bonded sand with 2 wt.% phenolic resin and an AFS GFN of 55. The sand was mixed in an industrial mixer and manually compacted into the pattern box. Three molds were prepared for the heat. Only one casting was utilized in this work.

A 3 kHz induction furnace, operating in an air atmosphere, was used to melt a 23 kg heat. The furnace was lined with a high alumina refractory. Table 1 lists the composition of the experimental alloy. The initial charge consisted of 1010 scrap. When the melt temperature reached 1650C (3002F), FeSi, electrolytic manganese, and graphite were introduced. The molten metal was then poured into a preheated magnesia fiber refractory lined ladle at 1740C (3164F). The castings were poured at 1620C (2948F) and then allowed to cool for 30 minutes before shakeout. These castings cooled overnight until they reached room temperature.

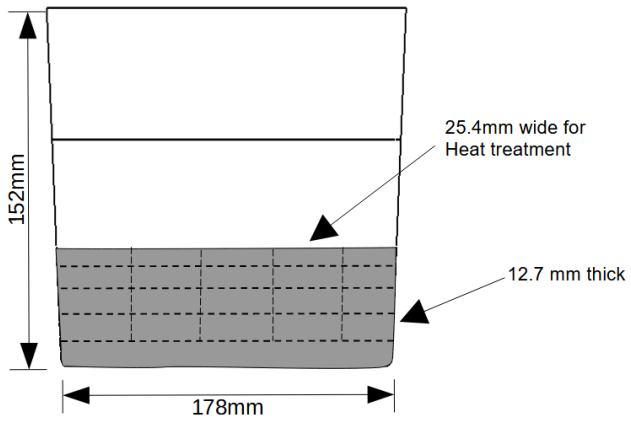

Figure 2. A 25mm thick, 152mm height, and 178mm wide Y-block casting was employed in this experiment.

Table 1. Chemical Composition of Q&P Steel (wt.%)

C	Si	Mn	Cr	Al	P	S
0.25	1.7	3.4	0.035	0.03	<0.005	0.011

Table 2. Heat Treatment Cycle Times

HT Cycle	Quench Time (min)	Partition Time (min)
15Q	15	-
30Q	30	-
60Q	60	-
15Q05P	15	05
15Q10P	15	10
15Q30P	15	30
15Q60P	15	60
30Q05P	30	05
30Q10P	30	10
30Q30P	30	30
30Q60P	30	60

The casting was then sectioned into 25.4 mm x 25.4 mm x 12.7 mm thick slices using a vertical bandsaw. Figure 2 depicts the locations within the casting where the samples were sectioned from. Each sample was stamped with a slice and location number for tracking their location in the original casting. Subsequently, the samples were randomly selected for the various heat treatments. All samples were heated in a muffle furnace at 800C (1472F) for 1 hour in air. The samples were quenched in an oil bath at 140C (284F). Some samples went through a partitioning stage using a molten salt bath at 420C (788F) in a muffle furnace. Table 2 lists the heat treatment (HT) cycles used for each sample and their label. Three samples were only quenched to determine structure evolution during quenching. These were then air cooled. After partitioning, the samples were allowed to cool to room temperature. The HT cycle label is used throughout this paper to refer to the samples. The authors only conducted the full Q&P process on samples with 15 and 30 minute quench times due to theories by other authors that extremely long quench times could lead to carbide precipitation.[18]

Post heat treatment, the surface on one side of each sample was ground using a belt grinder to remove surface oxidation and the decarburized layer. Rockwell C hardness testing was employed to measure the hardness of the HT specimens. Five hardness measurements were done for each sample. These measurements were approximately 3 mm apart.

After measuring the hardness, a metallurgical sample was cut from the side opposite of the hardness tested area. This was accomplished with a low-speed precision saw. The samples were mounted in a copper based conductive mounting compound. The specimens underwent grinding using SiC sandpaper with grit sizes of 320, 400, 600, 800, and 1200 using a semi-automatic polisher. Subsequent to the grinding process, polishing was executed using a 1µm polycrystalline diamond followed by a 0.05 µm alumina slurry. To reveal the microstructure, the specimens were etched with 3% Nital for a duration of 10-15 seconds. Optical microscopy images were then captured for analysis.

A 1 mm thick sample was also extracted from the center of each sample for X-ray diffraction (XRD) analysis. A Rigaku SmartLab diffractometer using Cu Kα radiation was employed. Scans were made in the 2θ range of 20° to 75° at a 3°/min. rate. Once scans were completed, phase identification and Rietveld refinement occurred in Profex 5.2.8.[19] Reference crystal structure data came from the Crystallography Open Database.[20]

RESULTS AND DISCUSSION

HARDNESS

Figure 3 shows the hardness measurements at the quenched stage for each quench time. The error bars in all plots are 95% confidence intervals. The data indicates that there is no statistical difference between quench times.

Figure 4 depicts the hardness measurements at 15 min. of quenching for each partition time. This trend shows no statistical difference between partition times. It was hypothesized that longer partition times might result in greater hardness due to the formation of transition carbides at longer times. This behavior has been suspected to occur.[5] However, the observed data does not support this. Hardness remained relatively uniform regardless of partition time.

The 30 min. quenched samples exhibited a different trend than the 15 min. quenched samples. At partition times longer than 5 min. hardness appeared to decrease. This decrease occurred at around 10 min. of partitioning and then remained stable (Figure 5). A similar trend in Q&P steels was reported by Gerdemann et al.[5]

This behavior may have been due to additional carbon diffusing into the retained austenite, further stabilizing it. This can lead to a reduction in the hardness of the martensite, as it becomes less carbon-rich.[1,2,3,5] The partitioning effect on hardness is less in this set of experiments than others in the literature.[1,3,22]

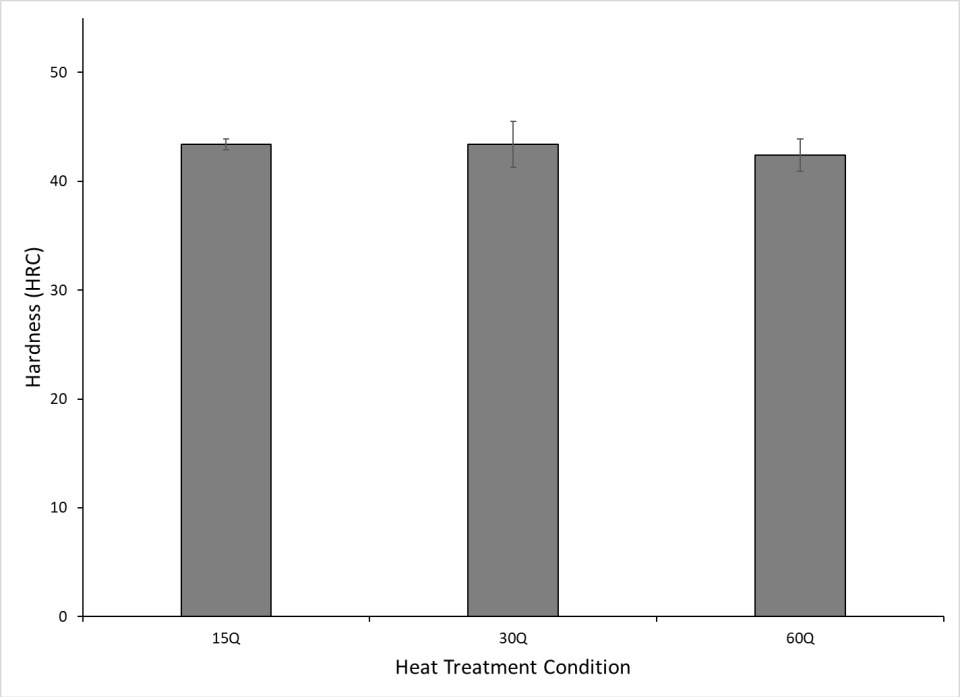

Figure 3. The hardness measurements at the quenched stage for each quench time.

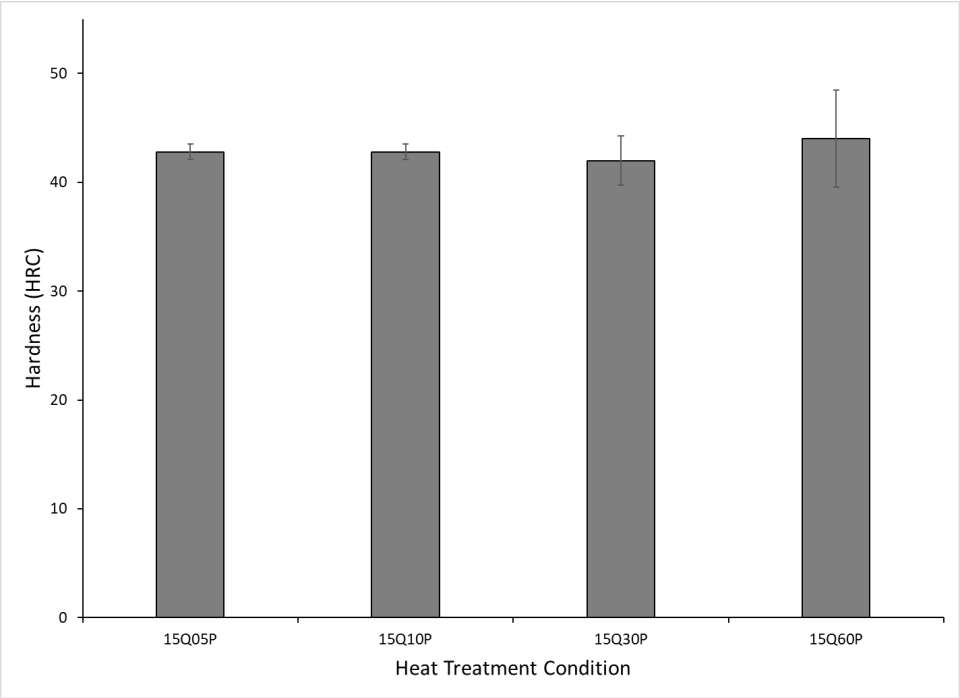

Figure 4. Hardness measurements for 15 min. quench at each partition.

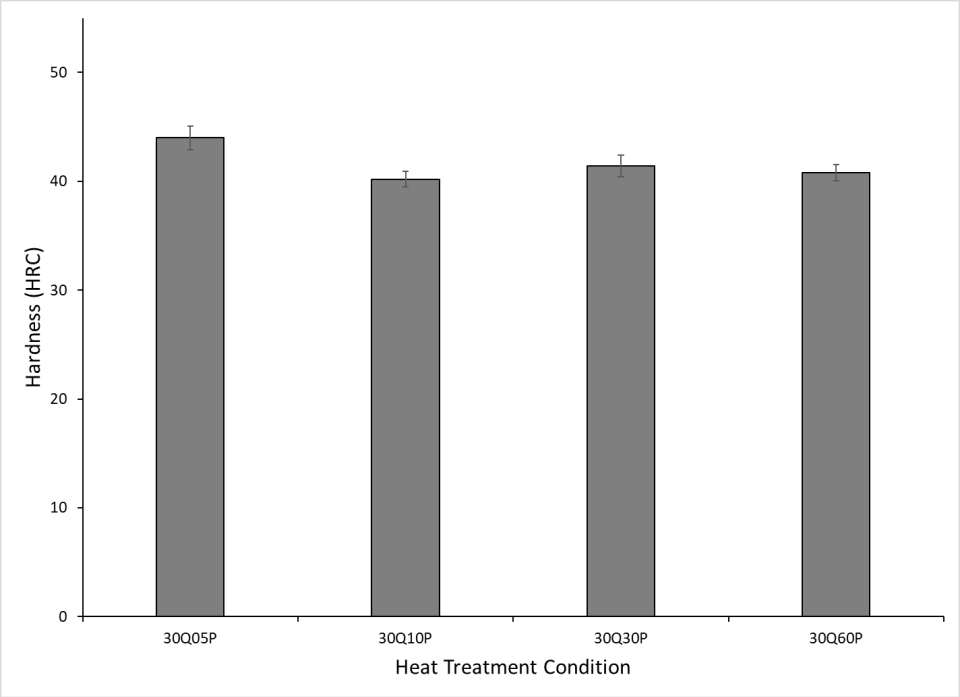

Figure 5. Hardness measurements for 30 min. quench at each partition.

MICROSTRUCTURE ANALYSIS

Figure 6 presents optical microscope images depicting the microstructures of the as-cast and quenched only samples. In Figure 6(A), the as-cast sample reveals a microstructure characterized by a primarily martensitic structure. The expected as-cast microstructure had been a combination of mostly ferrite with some martensite and retained austenite. The observed as-cast microstructure may be due to martensite formation during cooling after shakeout. The casting was still red hot at shakeout and the air cooling appears to have been sufficient to cause the primarily martensitic structure.

Figures 6(B) and (C) illustrate the microstructure of the samples quenched for 30 and 60 min., respectively, followed by cooling to room temperature. These microstructures exhibit the desired combination of martensite and retained austenite. The darker regions correspond to the martensite and the lighter areas are the retained austenite (Figures 6B and 6C). Notably, no carbides are observed at this stage of microstructural development in the optical microscope. A similar structure was also found in the 15 min. quenched sample so it was not presented. It appears that all the quench times were sufficient to form martensite within the structure.

Figure 7 comprises optical micrographs showing the resulting microstructure of the complete Q&P heat treatment at various intervals. Specifically, Figure 7(A) depicts the microstructure resulting from the 30Q5P parameters. In contrast, Figure 7(B) depicts the microstructure obtained from the 30Q60P sample. In both cases, the microstructural analysis reveals a microstructure containing martensite, retained austenite, and perhaps a carbide. The microstructures from all heat-treated samples showed a similar trend so only these two are shown for simplification.

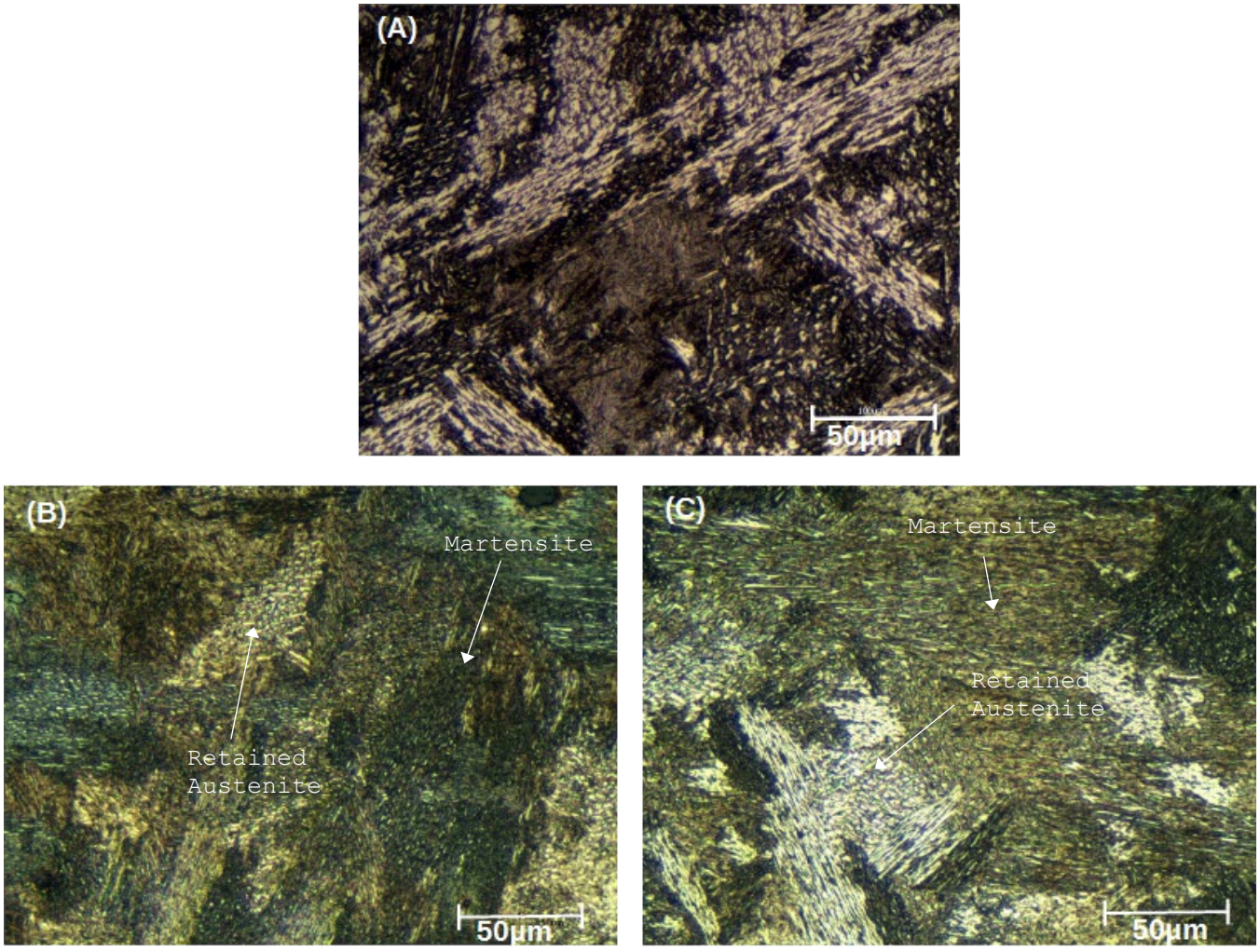

Figure 6. Optical micrographs (A) as-cast, (B) 30 min. quench, and (C) 60 min. quench.

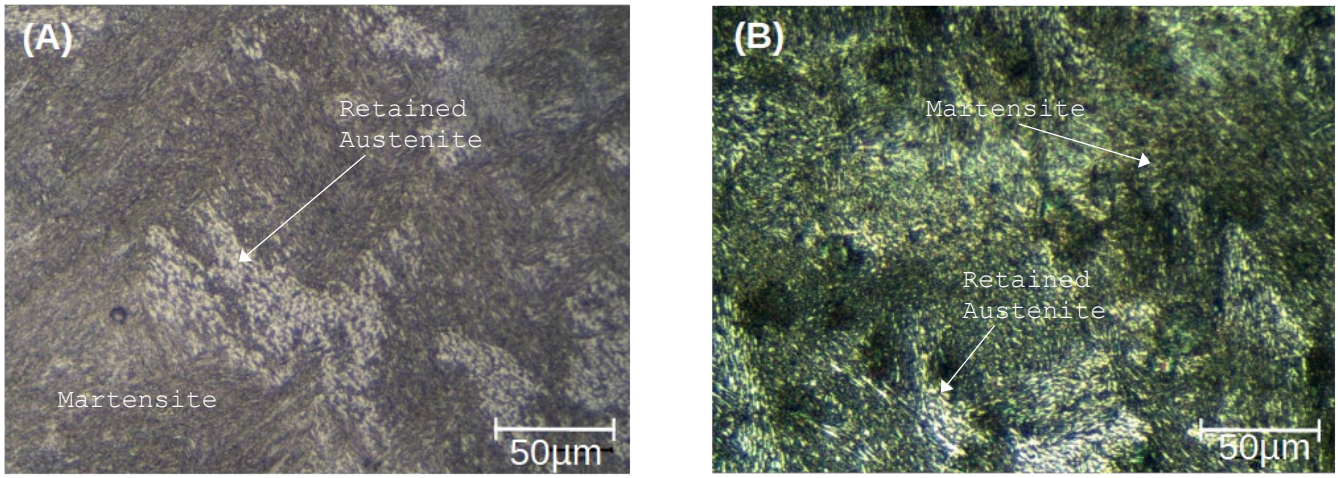

Figure 7. Optical micrographs of (A) 30 min. quench, 5 min. partition, (B) 30 min. quench, 60 min. partition.

QUANTITATIVE XRD

The XRD analysis of the as-cast sample found the microstructure consisted of 100% martensite (Figure 8). The large martensite fraction detected supports the earlier theory that the martensite probably formed while the casting air cooled. It is interesting to note that the body-centered cubic (BCC) form of martensite (α') was detected, not the typical ϵ-martensite form. This is likely due to the relatively low carbon content of the steel.

The XRD pattern of the quenched samples is provided in Figure 9. The XRD results for samples quenched for 15, 30, and 60 min. reveal a clear trend. The volume fraction of retained austenite rises as the quenching time increases (Figure 10). This trend was not expected since data previously published on this alloy indicated it should have a 10% austenite content within 6 sec.[23] At the start of the experiment, it was assumed that 30 min. would be sufficient for fully developing the target amount of austenite. The 60 min. quench was done simply to verify that assumption. However, the XRD data reveals it took that length of time in these samples to achieve a 10% austenite content. This behavior had been unexpected. The martensite transformation is athermal in nature so complete transformation based on only the temperature had been expected.[24- 26]A possible explanation for the observed behavior relates to the coarser structure of steel castings. It is well known that larger grain sizes during heat treating make martensite formation easier due to the larger diffusion distances involved.[24] In typical heat treatments, the material is quenched to room temperature where carbon mobility is limited. The quenching temperature employed in this work, and Q&P steels in general, means that some carbon mobility can be expected. It may be that initially larger amounts of martensite are formed due to the large diffusion distance and then as the steel remains at temperature atoms move to form the metastable fraction of austenite predicted for the alloy. Hence, the observed trend where the volume fraction of retained austenite increases with longer quenching time.

Figure 11 shows the XRD patterns of the fully Q&P treated samples. Rietveld quantitative analysis of the 15QxP series is presented in Figure 12. The XRD quantitative data indicates a retained austenite content similar to the 15Q sample (Figure 12). As partitioning time increases from 5 to 60 min., the amount of retained austenite appears constant (~4 vol.%). Precipitation of $M_{23}C_6$ carbide was also observed in the XRD data (Figures 11 and 12). Initially, the $M_{23}C_6$ carbide is approximately 2 vol. % and then increases to approximately 9.6 vol.% at 30 min. partition time and then decreases to 7.1 vol.% at the 60 min. partition time.

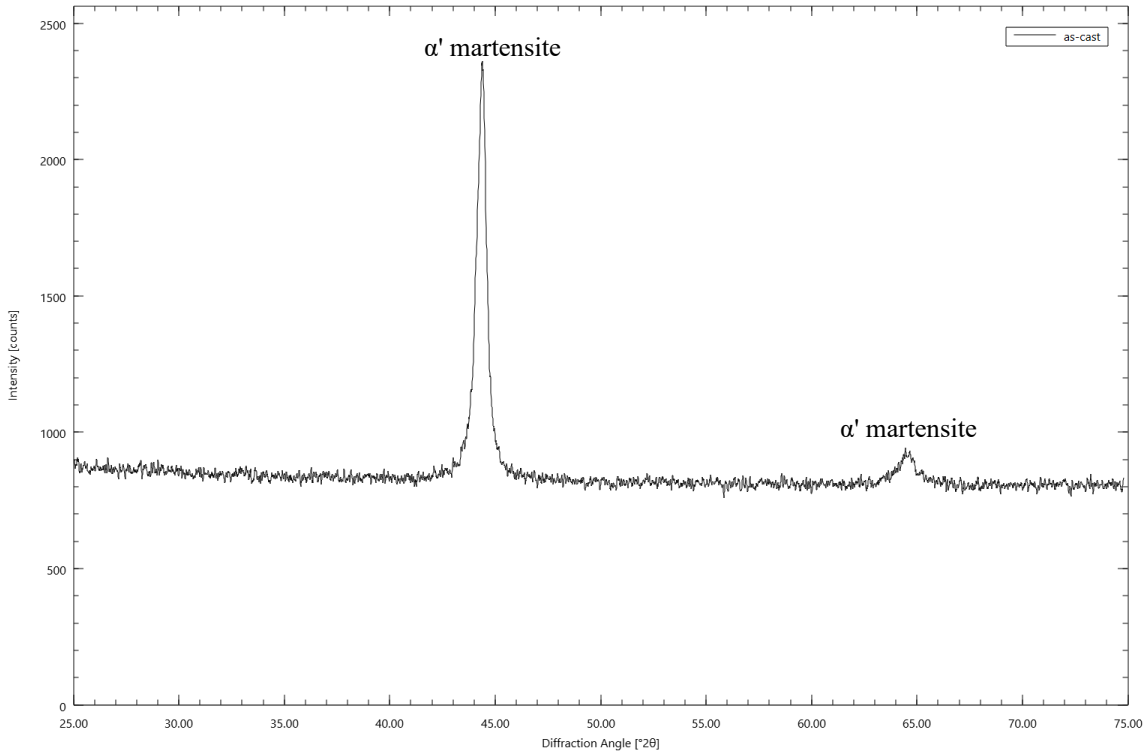

Figure 8. The XRD analysis of the as-cast sample found the microstructure consisted of 100% martensite.

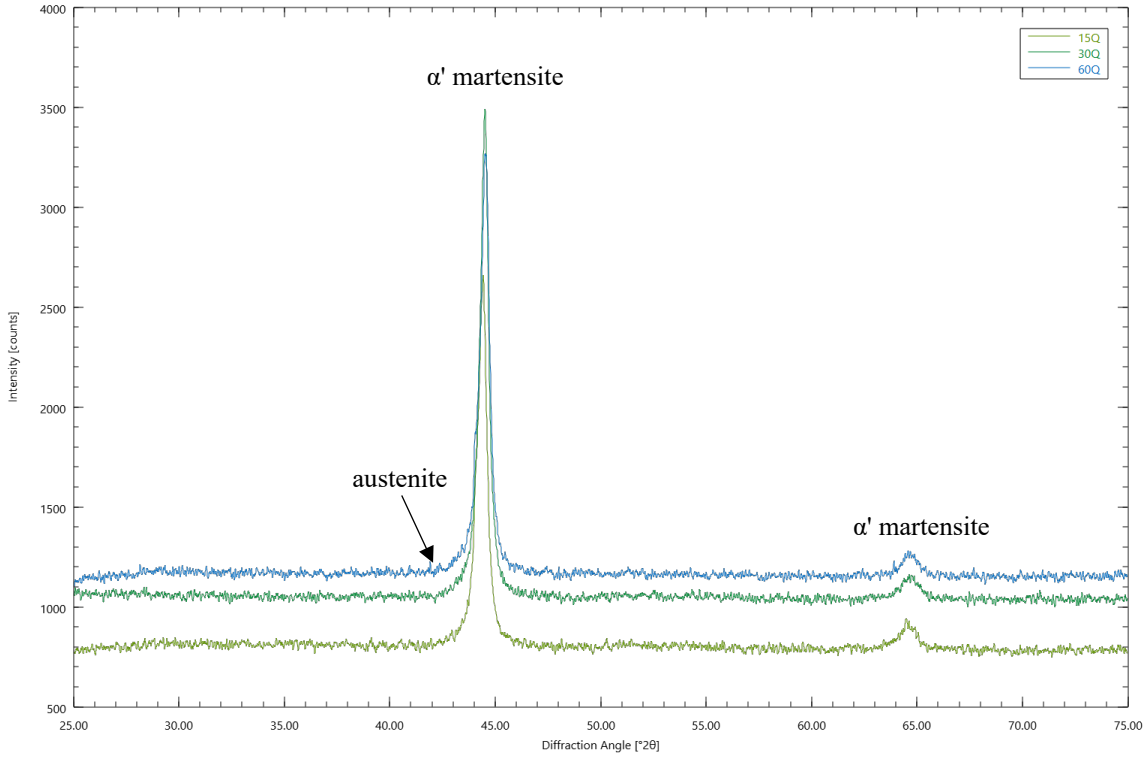

Figure 9. The XRD pattern of quenched samples at 15, 30 and 60 minutes.

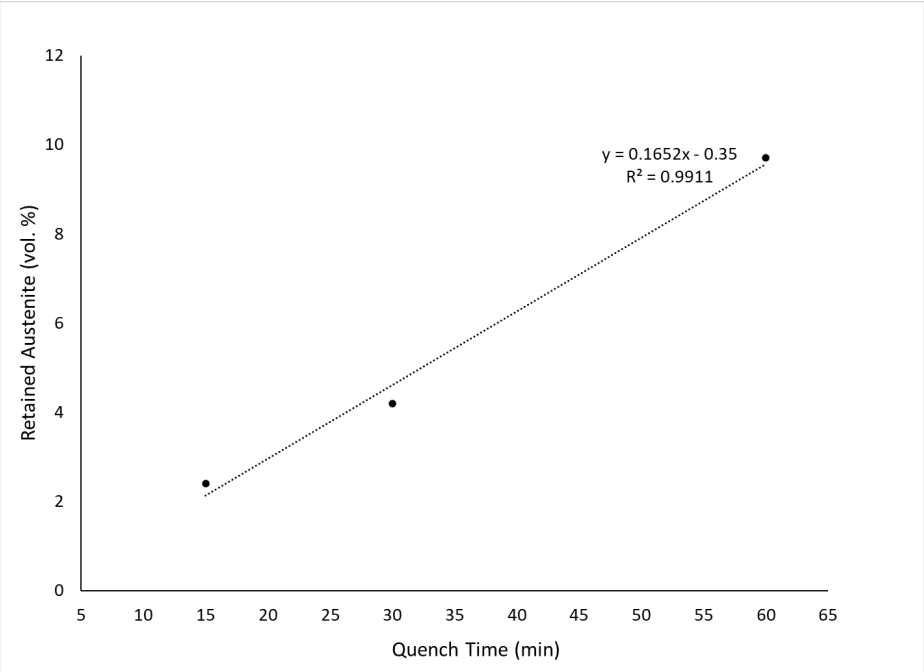

Figure 10. Volume fraction of retained austenite for only quench samples at 15, 30, and 60 minutes.

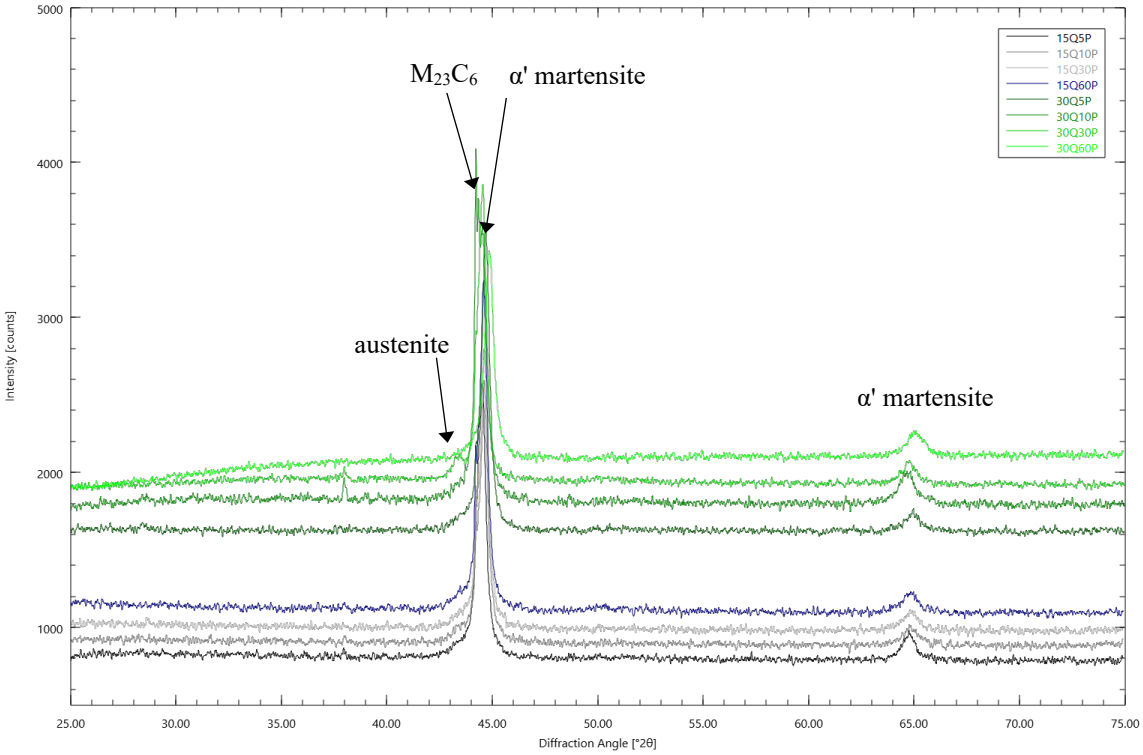

Figure 11. The XRD patterns of 15 and 30 minute quench and 5, 10, 30 and 60 minute partition times.

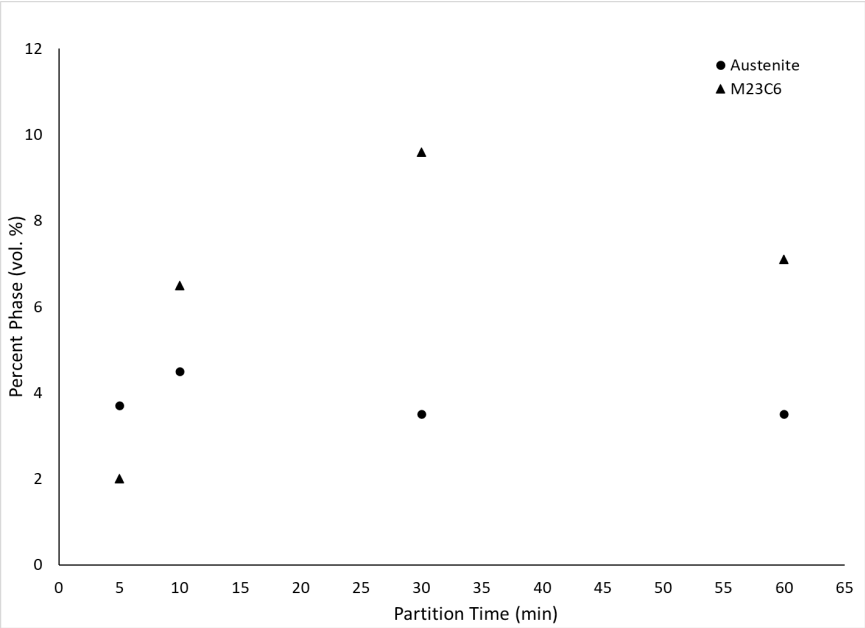

Figure 12. Volume fraction of retained austenite for 15 minute quench and 5, 10, 30 and 60 minute partition times.

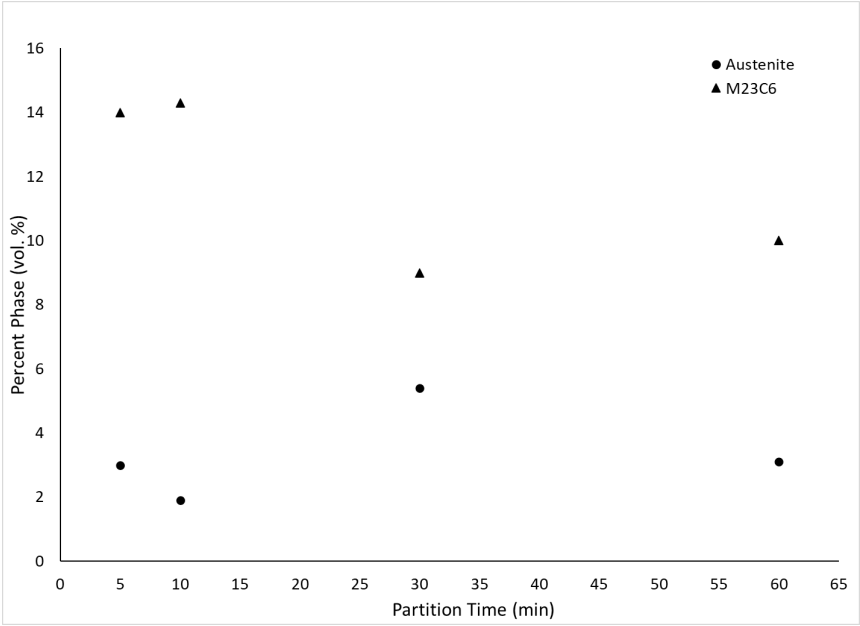

Figure 13.Volume fraction of retained austenite for 30 minute quench and 5, 10, 30 and 60 minute partition times.

Figure 13 depicts the phase evolution during partitioning for the 30QxP samples. The austenite content remains around 4 vol.% like the 15QxP series samples.
The formation of $M_{23}C_6$ carbides appears to initially be higher at this quench time and then decreases to a level similar to the 15Q60P sample after only 30 min. of partitioning. The cause of this behavior is not immediately apparent since no $M_{23}C_6$ carbide was detected when only quenching samples. Thus, it is not for a longer time at the quench temperature. Overall, it appears that an 8-10 vol.% $M_{23}C_6$ carbide content may be expected for this material and process combination. Additionally, a 30 min. partition appears to be sufficient for fully stabilizing the microstructure.

The lack of difference in hardness observed during testing was likely due to the high martensite fraction. At all heat treatments, this phase made up 85% to 95% of the microstructure. Additionally, the retrained austenite likely transformed to additional martensite during testing to the actual martensite content was over 90%. This phase is

extremely hard and caused the hardness to be relatively the same.

CONCLUSION

The experimental observations revealed that varying quenching times (15 min. and 30 min.) followed by partitioning at intervals of 5, 10, 30, and 60 min. resulted in relatively consistent hardness values across all samples. X-ray diffraction analysis quantified the volume fractions of martensite, retained austenite, and $M_{23}C_6$ carbides. highlighting the stability of retained austenite. The retained austenite remained stable at all partitioning times; however, the amount of $M_{23}C_6$ carbides required 30 minutes of partitioning time to stabilize.

The experiments also suggest that for thicker sections, longer quench times (~60 min.) are necessary to achieve the desired amount of retained austenite. This appears to be due to the coarser microstructure of steel castings. The larger grains assist the formation of martensite and additional time is required for the predicted amount of retained austenite to occur.

Overall, the Q&P process appears promising for cast steel applications which are desirable for critical performance in various industries. The experimental results show that the desired microstructure can be obtained in cast steels with section sizes similar to those in actual castings. Adjustments in the heat treatment cycles will be necessary to account for the longer times required to heat or cool these larger section sizes and coarser microstructures. However, the time scales required appear to be viable for industrial practice.

ACKNOWLEDGMENTS

The authors would like to acknowledge the assistance of Demitrios Cortez in assisting with the processing of the castings. The financial support of Western Michigan University is also greatly appreciated. Finally, they would like to thank Dr. Qingliu Wu for access to the X-ray diffractometer used in this work.

REFERENCES

1. Speer, J.G., Streicher, A.M., Matlock, D.K., Rizzo, F. & Krauss, G., "Quenching and Partitioning: A Fundamentally New Process to Create High Strength TRIP Sheet Microstructures," *Austenite Formation and Decomposition*, pp. 505–522 (2003).
2. Speer, J.G., Assunção, F.C.R., Matlock, D.K. & Edmonds, D.V., "The “quenching and partitioning” process: background and recent progress," *Materials Research*, vol. 8 (4), pp. 417–423 (2005).
3. Speer, J., Matlock, D.K., De Cooman, B.C. & Schroth, J.G., "Carbon Partitioning into Austenite after Martensite Transformation," *Acta Materialia*, vol. 51 (9), pp. 2611–2622 (2003).
4. Wang, L. & Speer, J.G., "Quenching and Partitioning Steel Heat Treatment," *Metallography, Microstructure, and Analysis*, vol. 2 (4), pp. 268–281 (2013).
5. Gerdemann, F., Speer, J.G. & Matlock, D.K., "Microstructure and Hardness of Steel Grade 9260 Heat-treated by the Quenching and Partitioning (Q&P) Process," *MS&T 2004 Conference Proceedings*, pp. 439–449 (2004).
6. Wendler, M., Ullrich, C., *et al.*, "Quenching and Partitioning (Q&P) Processing of Fully Austenitic Stainless Steels," *Acta Materialia*, vol. 133, pp. 346–355 (2017).
7. Cao, R., Liang, J., Li, F., Li, C. & Zhao, Z., "Intercritical Annealing Processing and a New Type of Quenching and Partitioning Processing, Actualized by Combining Intercritical Quenching and Tempering, for Medium Manganese Lightweight Steel," *Steel Research International*, vol. 91 (1), pp. 1900335 (2020).
8. Chen, P., Li, X. W., *et al.*, "Partitioning-related microstructure evolution and mechanical behavior in a δ-quenching and partitioning steel," *Journal of Materials Research and Technology*, vol. 17, pp. 1338–1348 (2022).
9. Zhang, K., Liu, P., Li, W., Ma, F., Guo, Z. & Rong, Y., "Enhancement of the Strenght and Ductility of Martensitic Steels by Carbon," *Materials Science and Engineering: A*, vol. 716, pp. 87–91 (2018).
10. He, B.B., Liu, L. & Huang, M.X., "Room-Temperature Quenching and Partitioning Steel," *Metallurgical and Materials Transactions A*, vol. 49 (8), pp. 3167–3172 (2018).
11. Wang, G.-T., Zhou, Y.-L., Wang, L.-J. & Liu, C.-M., "Study on Microstructures and Properties of Low-Carbon-Steel Heavy Plate Treated by Quenching and Dynamic Partitioning," *Journal of Materials Engineering and Performance*, vol. 31 (2), pp. 1195–1203 (2022).
12. Meng, L., Li, W., Shi, Q., Guo, H., Liang, W. & Lu, H., "Effect of Partitioning Treatment on the Microstructure and Properties of Low-carbon Ferritic Stainless Steel Treated by a Quenching and Partitioning Process," *Materials Science and Engineering: A*, vol. 851, pp. 143658 (2022).
13. Mohapatra, J. N., Dabbiru, S. K. & Balachandran, G., "Development of Ultra-high Strength Steel with a Versatile Range of Properties by Single Stage Quench Partitioning Process," *Transactions of the Indian Institute of Metals*, vol. 76 (7), pp. 1905–1913 (2023).

14. Mohammadi Zahrani, M., Ketabchi, M. & Ranjbarnodeh, E., "Microstructure Development and Mecanical Properties of a C-Mn-Si-Al-Cr Cold Rolled Steel Subjected to Quenching and Partitioning Treatment," *Journal of Materials Research and Technology*, vol. 22, pp. 2806–2818 (2023).
15. Wang, J., Qian, R., Yang, X., Zhong, Y. & Shang, C., "Effect of Segregation on the Microstructure and Properties of a Quenching and Partitioning Steel," *Materials Letters*, vol. 325, pp. 132815 (2022).
16. Lobo, J.A. & Geiger, G.H., "Thermodynamics of Carbon in Austenite and Fe-Mo Austenite," *Metallurgical Transactions A*, vol. 7 (8), pp. 1359–1364 (1976).
17. Lobo, J.A. & Geiger, G.H., "Thermodynamics and Solubility of Carbon in Ferrite and Ferritic Fe-Mo Alloys," *Metallurgical Transactions A*, vol. 7 (8), pp. 1347–1357 (1976).
18. Speer, J.G., De Moor, E. & Clarke, A.J., "Critical Assessment 7: Quenching and partitioning," *Materials Science and Technology*, vol. 31 (1), pp. 3–9 (2015).
19. Doebelin, N. & Kleeberg, R., "*Profex* : a graphical user interface for the Rietveld refinement program *BGMN*," *Journal of Applied Crystallography*, vol. 48 (5), pp. 1573–1580 (2015).
20. Vaitkus, A., Merkys, A., *et al.*, "A workflow for deriving chemical entities from crystallographic data and its application to the Crystallography Open Database," *Journal of Cheminformatics*, vol. 15 (1), pp. 123 (2023).
21. Vandijk, N., Butt, A., *et al.*, "Thermal stability of retained austenite in TRIP steels studied by synchrotron X-ray diffraction during cooling," *Acta Materialia*, vol. 53 (20), pp. 5439–5447 (2005).
22. Moor, E.D., Speer, J.G., Matlock, D.K., Kwak, J.-H. & Lee, S.-B., "Effect of Carbon and Manganese on the Quenching and Partitioning Response of CMnSi Steels," *ISIJ International*, vol. 51 (1), pp. 137–144 (2011).
23. Gao, P., Li, F., An, K., Zhao, Z., Chu, X. & Cui, H., "Microstructure and Deformation Mechanism of Si-strengthened Intercritically Annealed Quenching and Partitioning Steels," *Materials Characterization*, vol. 191, pp. 112145 (2022).
24. Hosford, W.F., "Physical Metallurgy," CRC Press/Taylor & Francis, Boca Raton, FL (2010).
25. Speer, J. & De Cooman, B., "Fundamentals of Steel Product Physical Metallurgy," Association of Iron & Steel Technology, Pittsburg, PA, (2011).
26. Song, C., Yu, H., Li, L., Zhou, T., Lu, J. & Liu, X., "The stability of retained austenite at different locations during straining of I&Q&P steel," *Materials Science and Engineering: A*, vol. 670, pp. 326–334 (2016).